Extended quark mean-field model for neutron stars

J. N. Hu,[2] A. Li,[1,3,*] H. Toki,[4] and W. Zuo[3,5]

[1]*Department of Astronomy and Institute of Theoretical Physics and Astrophysics, Xiamen University, Xiamen, Fujian 361005, China*
[2]*State Key Laboratory of Nuclear Physics and Technology, School of Physics, Peking University, Beijing 100871, China*
[3]*State Key Laboratory of Theoretical Physics, Institute of Theoretical Physics, Chinese Academy of Sciences, Beijing 100190, China*
[4]*Research Center for Nuclear Physics (RCNP), Osaka University, Ibaraki, Osaka 567-0047, Japan*
[5]*Institute of Modern Physics, Chinese Academy of Sciences, Lanzhou 730000, China*

(Received 16 July 2013; revised manuscript received 2 January 2014; published 5 February 2014)

We extend the quark mean-field (QMF) model to strangeness freedom to study the properties of hyperons (Λ, Σ, Ξ) in infinite baryon matter and neutron star properties. The baryon-scalar meson couplings in the QMF model are determined self-consistently from the quark level, where the quark confinement is taken into account in terms of a scalar-vector harmonic oscillator potential. The strength of such confinement potential for u,d quarks is constrained by the properties of finite nuclei, while that for an s quark is limited by the properties of nuclei with a Λ hyperon. These two strengths are not the same, which represents the SU(3) symmetry breaking effectively in the QMF model. Also, we use an enhanced Σ coupling with the vector meson, and both Σ and Ξ hyperon potentials can be properly described in the model. The effects of the SU(3) symmetry breaking on the neutron star structures are then studied. We find that the SU(3) breaking shifts the hyperon onset density earlier and makes hyperons more abundant in the star, in comparison with the results of the SU(3) symmetry case. However, it has little effect on the star's maximum mass. The maximum masses are found to be $1.62M_\odot$ with hyperons and $1.88M_\odot$ without hyperons. The present neutron star model is shown to have limitations in explaining the recently measured heavy pulsars around $2M_\odot$.

DOI: 10.1103/PhysRevC.89.025802 PACS number(s): 24.10.Jv, 26.60.−c, 21.60.−n, 97.60.Jd

I. INTRODUCTION

Hyperon-meson couplings and their repulsive and/or attractive natures are crucial for hypernuclei physics and neutron star (NS) properties in relativistic effective field theories, such as the relativistic mean-field (RMF) model [1–13], the quark-meson-coupling (QMC) model [14–23], and the quark mean-field (QMF) model [24–33].

For the case of hypernuclei, they essentially determine whether there is a possibility of the production of the relevant hypernuclei in the laboratory. For example, Λ-nucleus [34] and $\Lambda\Lambda$ interactions [35] have long been known as attractive interactions, while an opposite sign is indicated for the Σ-nucleus interaction (see, e.g., Refs. [1,2]). Recently an attractive nature has been suggested for the Ξ-nucleus interaction [36,37]. For example, the BNL-E885 Collaboration measured the missing mass spectra for the ^{12}C(K^-,K^+)X reaction [36], and reasonable agreement between this data and theory is realized by assuming a Ξ-nucleus Wood-Saxon potential with a depth of −14 MeV. Within the realistic Nijmegen ESC08 baryon-baryon interaction models [38], the Ξ nucleus for low densities is also found to be attractive enough to produce Ξ hypernuclear states in finite systems [39,40]. Presently, Ξ hypernulcei have been planned for several radiation active beam factories around the world [for example, in the Japan Proton Accelerator Research Complex (J-PARC)]. They are very promising objects that will contribute significantly to understanding nuclear structure and interactions in $S = -2$ systems, giving us more insight into the general understanding of the baryon-baryon interaction, as many successfully produced Λ hypernuclei have done.

Therefore any effective many-body theory should respect those hypernuclei data before proceeding to other sophisticated studies. The adopted hyperon-meson couplings need to at least reproduce unambiguous hypernuclear data, for example, the single Λ potential well depth in symmetric nuclear matter, $U_\Lambda^{(N)} \sim -30$ MeV [34]. Specifically, the usually employed flavor SU(3) symmetry, as a way to determine hyperon couplings from the corresponding nucleon coupling, may have modified [3], since the construction of realistic hyperon interactions has already been performed based on a broken-flavor SU(3) symmetry [38].

Furthermore, one can more microscopically constrain the hyperon-scalar couplings consistently from the quark level. Regarding this issue, the QMC model and the QMF model can serve equally well in a different manner. These two models have the same root from the Guichon model proposed in 1988 [41], where the meson fields couple not with nucleons, as in the RMF theory [42], but directly with the quarks in nucleons. Then the nucleon properties change according to the strengths of the mean fields acting on the quarks, allowing us to study properties of nuclear many-body systems directly from a phenomenological model of the quark-quark confinement potential. Before doing that, a nucleon model is necessary. Two nucleon models available, namely, the MIT bag model [43] and the constituent quark model [44], were finally developed as the QMC model and the QMF model, respectively. For a more detailed comparison of these two models, we refer to Ref. [24]. Briefly, the first model assumes the nucleon constitutes bare quarks in the perturbative vacuum, i.e., current quarks, with a bag constant to account for the energy difference

*liang@xmu.edu.cn

between the perturbative vacuum and the nonperturbative vacuum, while in the second model, the nucleon is described in terms of constituent quarks which couple with mesons and gluons.

The QMC model has been generalized by Fleck *et al*. [14] and Saito and Thomas [15], and employed extensively in many calculations of finite nuclei and infinite nuclear matter [16–23]. The QMF model has been applied to nuclear matter [24] and then to finite nuclei [25]. More recently, Wang *et al*. [26] included the chiral symmetry in the QMF model, and it was then called by authors as "the chiral SU(3) QMF model" or "a QMC model based on $SU(3)_L \times SU(3)_R$ symmetry." In this chiral SU(3) QMF model [26], an effective chiral Lagrangian was introduced with an explicit symmetry-breaking term for reproducing the reasonable hyperon potentials in hadronic matter. They use two parameters, h_1 and h_2, to achieve an overall good agreement of all the hyperon potentials for the four types of quark confinement potentials. In Ref. [27], Wang and co-workers further introduced a linear definition of the effective baryon mass to postpone the critical density of a zero effective baryon mass (i.e., achieve a slower decrease of mass at high density) than the usual square root ansatz. This linear definition of the effective mass was applied to a NS study in Ref. [28], together with a scalar confining potential. In their calculation, the values of a single hyperon in nuclear matter are obtained as $U_\Lambda^{(N)} = U_\Sigma^{(N)} = -28$ MeV and $U_\Xi^{(N)} = 8$ MeV. They finally got a maximum mass of $1.45M_\odot$ ($1.7M_\odot$) with (without) hyperons in the star's dense core.

In the present work, based on our previous studies [24,25], an extended-QMF (EQMF) model is formulated to the study of the properties of hyperons (Λ, Σ, Ξ) in infinite nuclear matter and NSs. Special efforts are devoted to effectively introduce the SU(3) symmetry breaking in a different way than Ref. [26]. That is, we do not include an explicit symmetry-breaking term [26] in the effective Lagrangian. Instead, we assume a different confining strength for the s quark with the u,d quarks in the corresponding Dirac equations (under the influence of the meson mean fields). Also, the confining strength of the u,d quarks is constrained from finite nuclei properties and that of the s quark by the well-established empirical value of $U_\Lambda^{(N)} \sim -30$ MeV. The presently expected single Σ potential of $U_\Lambda^{(N)} \sim 30$ MeV [1] is then used to determine the Σ coupling with the vector ω meson. Namely, a slightly larger $\Sigma-\omega$ coupling was taken, as compared to $\Lambda-\omega$ coupling, to simulate the additional repulsion on the Σ-nucleon channel.

We use a scalar-vector type of harmonic oscillator potential for the confinement instead of the scalar one used in Ref. [28], since a denser matter can be achieved before the effective mass drop to zero (shown in Ref. [24]), which serves our purpose of studying NSs with hyperon cores. Also, based on those fairly developed model calculations, we also try to emphasize some general features of relativistic models widely used in the literature and contribute a more comprehensive understanding of effective many-body theories. Moreover, since we do connect the theoretical NS maximum mass with the underlying quark-quark confining potentials, an analysis of their dependence is feasible, and we also discuss the theoretical implications to the recent NS mass measurements.

The paper is organized as follows. In Sec. II we demonstrate how the EQMF model is obtained by incorporating all eight octet baryons, including a differently modeled s-quark potential strength, the consistent determination of baryon-scalar coupling from the quark level, and the consequential description of NS properties. The numerical results and discussion are given in Sec. III. Finally, Sec. IV contains the main conclusions and future perspectives of this work.

II. FORMALISM

We shall begin with a possible Lagrangian [24,25,29,45] of the quark many-body system, taking into account the nonperturbative gluon dynamics of spontaneous chiral symmetry breaking and quark confinement. In this effective Lagrangian, we construct the interaction between baryons through the meson fields σ, ω, and ρ. The nucleon and meson fields are treated as a mean-field approximation. The inclusion of other mesons is straightforward. Then, in the second step, we solve the entire baryon system by knowing the individual baryon properties due to the presence of the mean fields.

In the first step, octet baryons (N,Λ,Σ,Ξ) are described as composites of three quarks satisfying the Dirac equations with confinement potentials. The Dirac equations for constituent quarks can be written as

$$\left[-i\vec{\alpha}\cdot\vec{\nabla}+\beta m_i^*+\beta\chi_c^i\right]q^i(r)=e_i^*q^i(r), \tag{1}$$

where $i = q,s$ with the subscript q denote as u or d quark. The quark masses, $m_q = 313$ MeV and $m_s = 490$ MeV, are modified to $m_i^* = m_i + g_\sigma^i\sigma$ due to the presence of the σ mean field. $e_i^* = e_i - g_\omega^i\omega - g_\rho^i\rho\tau_3^i$, with σ, ω, and ρ being the mean fields at the middle of the baryon, where e_i is the energy of the quark under the influence of the σ, ω, and ρ mean fields. The confinement potential is chosen to be a scalar-vector confinement, as $\chi_c^i = \frac{1}{2}k^i r^2(1+\gamma^0)/2$. For the potential strength, a previous study [25] of Λ hypernuclei chose $k^q = k^s = 700\ \mathrm{MeV/fm^2}$, applying the SU(3) symmetry. We here respect the difference between u,s quarks and the s quark, and adjust k^s to properly reproduce the hypernuclei experimental data. We then generate the mass difference among baryons by taking into account the spin correlations $E_B^* = \sum_i e_i^* + E_{\rm spin}^B$, where $B = N,\Lambda,\Sigma,\Xi$. The spin correlations are fixed by fitting the baryon masses in free space, namely, $M_N = 939$ MeV, $M_\Lambda = 1116$ MeV, $M_\Sigma = 1192$ MeV, and $M_\Xi = 1318$ MeV. We get $E_{\rm spin}^N = 795$ MeV, $E_{\rm spin}^\Lambda = 821$ MeV, $E_{\rm spin}^\Sigma = 759$ MeV, and $E_{\rm spin}^\Xi = 825$ MeV at $k^s = 1100\ \mathrm{MeV/fm^2}$, where the single Λ potential is $U_\Lambda^{(N)} \sim -30$ MeV. In addition, the spurious center-of-mass motion is removed in the usual square root method as $M_B^* = \sqrt{E_B^{*2} - \langle p_{\rm c.m.}^2\rangle}$.

By solving the above Dirac equations, we work out the change of the baryon mass M_B^* as a function of the quark mass correction $\delta m_q = m_q - m_q^*$, which is used as input in the next step of the study of nuclear many-body systems, that is, infinite strange nuclear matter. Baryons inside the matter interact through exchange of σ,ω,ρ mesons, and the corresponding Lagrangian can be written as

$$\begin{aligned}\mathcal{L}_{\rm QMF} = &\sum_B \bar{\psi}_B[i\gamma_\mu\partial^\mu - M_B^* - g_{\omega B}\omega\gamma^0 - g_{\rho B}\rho\tau_{3B}\gamma^0]\psi_B \\ &- \frac{1}{2}(\nabla\sigma)^2 - \frac{1}{2}m_\sigma^2\sigma^2 - \frac{1}{4}g_3\sigma^4 \\ &+ \frac{1}{2}(\nabla\omega)^2 + \frac{1}{2}m_\omega^2\omega^2 + \frac{1}{4}c_3\omega^4 \\ &+ \frac{1}{2}(\nabla\rho)^2 + \frac{1}{2}m_\rho^2\rho^2,\end{aligned} \tag{2}$$

where ψ_B are the Dirac spinors of baryon B, and τ_{3B} is the corresponding isospin projection. m_σ, m_ω, and m_ρ are the meson masses. The mean-field approximation has been adopted for the exchanged σ, ω, and ρ mesons, while the mean-field values of these mesons are denoted by σ, ω, and ρ, respectively. The contribution of the σ meson is contained in M_B^*, and ω and ρ mesons couple to baryons with the following coupling constants:

$$g_{\omega N} = 3g_\omega^q, \quad g_{\omega\Lambda} = cg_{\omega\Sigma} = 2g_\omega^q, \quad g_{\omega\Xi} = g_\omega^q, \tag{3}$$

$$g_{\rho N} = g_\rho^q, \quad g_{\rho\Lambda} = 0, \quad g_{\rho\Sigma} = 2g_\rho^q, \quad g_{\rho\Xi} = g_\rho^q. \tag{4}$$

The basic parameters are the quark-meson couplings (g_σ^q, g_ω^q, and g_ρ^q), the nonlinear self-coupling constants (g_3 and c_3), and the mass of the σ meson (m_σ), which are given in Ref. [24] with $k^q = 700\ \mathrm{MeV/fm^{-2}}$. The saturation properties of nuclear matter with such a parameter set are listed in Table I. As done in our previous work [45], a factor c is introduced before $g_{\omega\Sigma}$ for a large $\Sigma-\omega$ coupling. From reproducing the presently expected single Σ potential $U_\Sigma^{(N)} = 30$ MeV at nuclear saturation density [1], we choose $c = 0.785$ (0.772) for $k^s = 700\ \mathrm{MeV/fm^{-2}}$ ($1100\ \mathrm{MeV/fm^{-2}}$). When $c = 1$ it goes back to the quark counting rule usually employed.

For infinite matter, introducing the mean-field approximation, we can write the equations of motion from the Lagrangian given in Eq. (2) as

$$m_\sigma^2\sigma + g_3\sigma^3 = \sum_B \frac{\partial M_B^*}{\partial\sigma}\frac{2J_B+1}{2}\rho_B^s, \tag{5}$$

$$m_\omega^2\omega + c_3\omega^3 = \sum_B g_{\omega B}\frac{2J_B+1}{2}\rho_B, \tag{6}$$

$$m_\rho^2\rho = \sum_B g_{\rho B}I_{3B}\frac{2J_B+1}{2}\rho_B, \tag{7}$$

TABLE I. Saturation properties of nuclear matter used to determined the free parameters (g_σ^q, g_ω^q, g_ρ^q, g_3, c_3, m_σ) in the present model. The saturation density and the energy per particle are denoted by ρ_0 and E/A, and the incompressibility by K, the effective mass by M_n^*, the symmetry energy by $a_{\rm sym}$.

ρ_0 ($\mathrm{fm^{-3}}$)	E/A (MeV)	K (MeV)	M_n^*/M_n	$a_{\rm sym}$ (MeV)
0.145	–16.3	280	0.63	35

where J_B and I_{3B} denote the spin and the isospin projection of baryon B, and the baryon-scalar density ρ_B^s is defined as

$$\rho_B^s = \frac{1}{\pi^2}\int_0^{k_B} dk\, k^2 \frac{M_B^*}{\sqrt{M_B^{*2}+k_B^2}}, \tag{8}$$

with k_B the Fermi momentum of the baryon species B. The total baryon density is calculated as $\rho = \rho_N + \rho_\Lambda + \rho_\Sigma + \rho_\Xi$.

To add leptons $L_l = \sum_{L=e,\mu}\overline{\psi}_L(i\gamma^\mu\partial_\mu - m_L)\psi_L$ to the above Lagrangian of hadronic matter [Eq. (2)], the charge neutrality requires

$$\rho_p + \rho_{\Sigma^+} = \rho_e + \rho_\mu + \rho_{\Sigma^-} + \rho_{\Xi^-}, \tag{9}$$

and equilibrium under the weak process (B_1 and B_2 denote baryons)

$$B_1 \to B_2 + L \qquad B_2 + L \to B_1$$

leads to the following relations among the involved chemical potentials:

$$\begin{aligned}&\mu_p = \mu_{\Sigma^+} = \mu_n - \mu_e, \quad \mu_\Lambda = \mu_{\Sigma^0} = \mu_{\Xi^0} = \mu_n, \\ &\mu_{\Sigma^-} = \mu_{\Xi^-} = \mu_n + \mu_e, \quad \mu_\mu = \mu_e,\end{aligned} \tag{10}$$

where μ_i is the chemical potential of species i.

We solve the coupled Eqs. (5), (6), (7), (9), and (10) at a given baryon density ρ, with the effective masses M_B^* obtained at the quark level. The equation of state (EoS) of the system can be calculated in the standard way. The stable configurations of a NS then can be obtained from the well-known hydrostatic equilibrium equations of Tolman, Oppenheimer, and Volkoff [46–48] for the pressure P and the enclosed mass m,

$$\frac{dP(r)}{dr} = -\frac{Gm(r)\mathcal{E}(r)}{r^2}\frac{\left[1+\frac{P(r)}{\mathcal{E}(r)}\right]\left[1+\frac{4\pi r^3P(r)}{m(r)}\right]}{1-\frac{2Gm(r)}{r}}, \tag{11}$$

$$\frac{dm(r)}{dr} = 4\pi r^2\mathcal{E}(r), \tag{12}$$

once the EoS $P(\mathcal{E})$ is specified, $\mathcal{E}$ being the total energy density (G is the gravitational constant). For a chosen central value of the energy density, the numerical integration of Eqs. (11) and (12) provides the mass-radius relation. For the description of the NS crust, we have joined the hadronic EoSs above described with the ones by Negele and Vautherin [49] in the medium-density regime ($0.001\ \mathrm{fm^{-3}} < \rho < 0.08\ \mathrm{fm^{-3}}$), and the ones by Feynman-Metropolis-Teller [50] and Baym-Pethick-Sutherland [51] for the outer crust ($\rho < 0.001\ \mathrm{fm^{-3}}$).

III. RESULTS

The potential strength of strange quark k^s must be equal to the strength of the u,d quark k^q if the SU(3) symmetry is considered. However, the SU(3) symmetry is not strictly conserved in nuclear physics, e.g., there is a mass difference between the Λ and Σ hyperon. Therefore the strange potential strength k^s will differ from the u,d quark case to take the effect of SU(3) symmetry breaking. k^q in the QMF model is determined by the ground-state properties of finite nuclei. Similarly, the magnitude of k^s can be extracted from the properties of hypernulcei, such as Λ hypernuclei, which is well

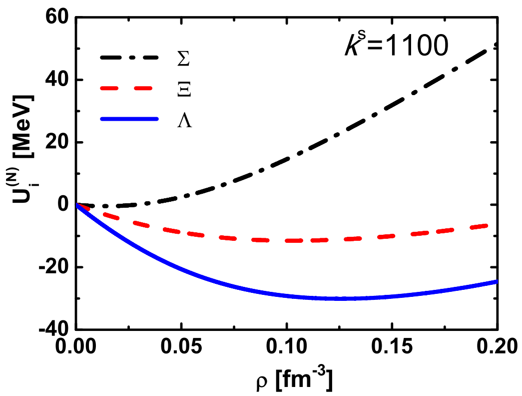

FIG. 1. (Color online) Single hyperon potentials $U_i^{(N)}$ as a function of density.

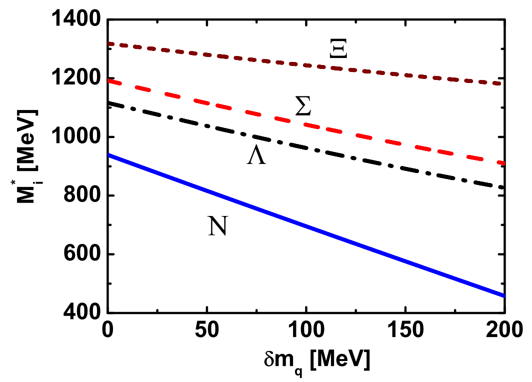

FIG. 2. (Color online) Effective baryon mass M_B^* as a function of the quark mass correction $\delta m_q = m_q - m_q^* = -g_\sigma^i \sigma$.

known in the strangeness physics. Its single-particle potential $U_\Lambda^{(N)}$ is around -30 MeV at nuclear saturation density. With such a constraint, we can choose the strange potential strength in the QMF model as $k^s = 1100\ \text{MeV/fm}^2$, which can generate the single Λ potential as $U_\Lambda^{(N)} = -29.64$ MeV at the saturation density $\rho = 0.145\ \text{fm}^{-3}$. This value is only $U_\Lambda^{(N)} = -25$ MeV when an equal value of $k^q = k^s = 700\ \text{MeV/fm}^2$ is chosen, as done in the previous study [25]. Meanwhile, we have checked that a reasonable description of baryon radii at around 0.6 fm is fulfilled.

In Fig. 1, the single hyperon (Λ, Σ, Ξ) potentials as a function of density are plotted with $k^s = 1100\ \text{MeV/fm}^2$. With density increasing, the single hyperon potentials are reduced the same as in the nucleon case, which is caused by the repulsive effect being stronger at high density. Furthermore, it is possible that the Ξ hypernuclei exist from our attractive Ξ potential, although such a bound state is a little bit weak at about 10 MeV, consistent with the experiments [36]. However, we notice that in the study of the SU(3) QMF model [28], a repulsive Ξ potential is obtained with $U_\Xi^{(N)} = 8$ MeV. As for the Σ potential, it is always repulsive, as caused by the use of slightly larger ω coupling strength. This is consistent with the experimental facts that no middle and heavier mass Σ hypernuclei have been found. The different hyperon potentials will manifest themselves in the relevant fractions of the stellar matter, as shown later.

Once the strange potential strength k^s is known, we can calculate the effective baryon mass M_B^* by solving the Dirac equation, namely, Eq. (1). The baryon masses M_B^* of Λ, Σ, and Ξ are given in Fig. 2 as functions of the quark mass correction. They are almost linear with the quark mass correction. Such behavior is strongly dependent on the form of quark potential, as shown in Ref. [24], and a linear relation is expected if a scalar-vector confining potential is employed. The hyperons in a many-body system will be influenced by the surrounding hyperons and nucleons; this is reflected in the effective hyperon masses shown here.

In the QMF model, the hadron part is dealt with by the RMF theory [42]. The interactions between baryons in the RMF theory are provided by meson exchanges. The coupling between σ mesons and baryons can be extracted from the baryon structure in the QMF model. They are strongly dependent on the baryon effective mass ∂M_B^*, as defined by $g_{\sigma B} = \partial M_B^* / \partial \sigma$. The ratios of $g_{\sigma\Lambda}$, $g_{\sigma\Sigma}$, $g_{\sigma\Xi}$ to $g_{\sigma N}$ are shown in Fig. 3 as a function of the total baryon density ρ for β equilibrium matter. At very low density, these ratios almost satisfy the quark counting rules, approaching 2/3 for Λ, Σ and 1/3 for Ξ, while with the increase of density all of them decrease steadily. This density-dependent behavior shows that the effect of a strange quark is weaker at high densities. Furthermore, we also notice that there is a small difference between the ratios of Λ and Σ, indicating the SU(3) symmetry breaking.

Solving the β equilibrium conditions in NS matter, we obtain the fraction of species i, $Y_i = \rho_i/\rho$, as a function of total baryon density ρ, as given in Fig. 4. At the low-density region (until $\rho < 0.21\ \text{fm}^{-3}$), the proton fraction $\frac{\rho_p}{\rho_n + \rho_p}$ is well below 1/9, which fulfills the astrophysical observations that direct URCA cooling does not occur at densities which are too low.

With the properly chosen Λ, Σ, and Ξ hyperon potentials, Λ is the first hyperon appearing at $\rho = 0.34\ \text{fm}^{-3}$, which is lower than the hyperon from the SU(3) symmetry calculation, 0.40 fm $^{-3}$. Namely, Λ hyperons appear earlier in the SU(3)-breaking case, as a result of a larger Λ-nucleon attraction.

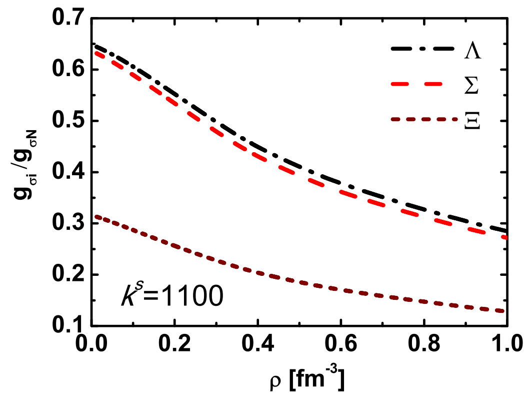

FIG. 3. (Color online) $g_{\sigma B}/g_{\sigma N}$ as a function of the baryon density ρ for β equilibrium matter, with $g_{\sigma B}$ defined by $\partial M_B^*/\partial\sigma$ in the present QMF model.

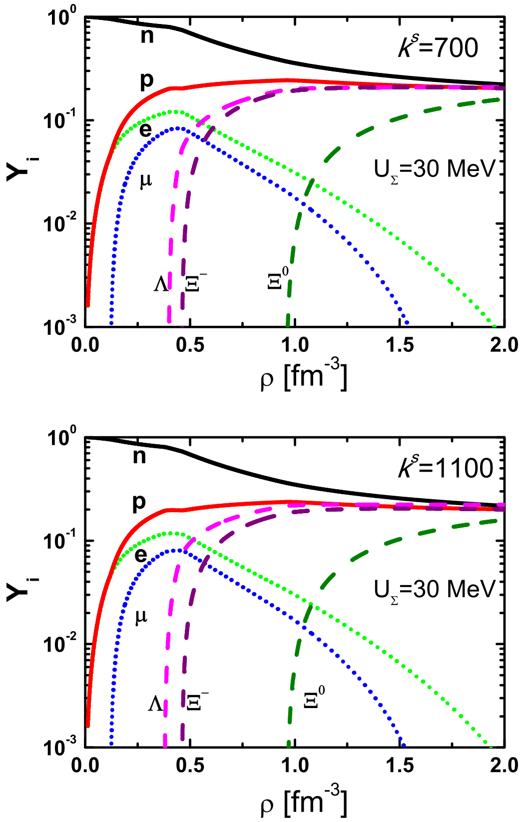

FIG. 4. (Color online) Fractions of leptons and baryons in NS matter are shown as a function of total baryon density, for both (upper panel) $k^s = 700$ MeV/fm^2 and (lower panel) $k^s = 1100$ MeV/fm^2 cases.

Then Ξ^- hyperons appear at $\rho = 0.46$ fm^{-3}, followed by Ξ^0 hyperons at $\rho = 0.96$ fm^{-3}. These two values do not change much whether we choose the SU(3) breaking potential or the SU(3) symmetry. The fractions of hyperons increase with density. Above $\rho > 1.25$ fm^{-3}, the fractions of Λ and Ξ^- are almost the same as the fractions of protons and neutrons. Σ^-, however, will not appear until very high density, up to 2.0 fm^{-3}. The appearing hyperon sequences are essentially different from the previous calculations using the quark counting rule for $\Sigma - \omega$ coupling [13], where Σ^- would be the first hyperon appearing at a similar density of Λ, as is also the case for the SU(3) QMF model [28].

We also show the pressure of β-equilibrated matter as a function of energy density in Fig. 5. The solid curve represents the EoS including the hyperon, and the dot-dashed curve is the EoS without hyperons. The EoS becomes softer after the presence of the strangeness freedom.

The NS properties are calculated by using the EoSs with or without hyperons obtained from the EQMF theory. The NS mass-radius relations are plotted in Fig. 6. It is found that the maximum mass of the NSs, including hyperons, is around $1.62M_\odot$, while it is around $1.88M_\odot$ without hyperons. Those values are larger than the corresponding results in the SU(3) QMF model mentioned before. However, both of them could not explain the observations of $2M_\odot$ NSs [52]. Our

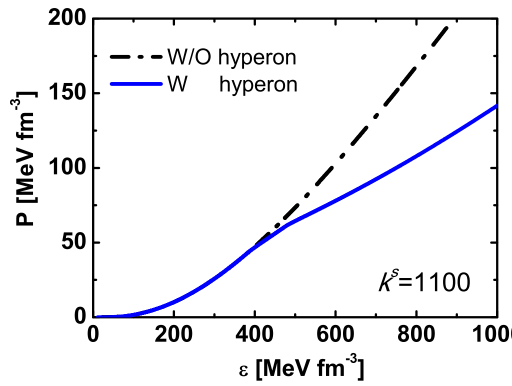

FIG. 5. (Color online) Pressures for β-equilibrated matter are shown as a function of the energy density, for cases with or without hyperons.

results are consistent with the conventional RMF calculations, including hyperons [1,2,4–6,13,53], and microscopic studies [54–56] based on developed realistic baryon-baryon interactions [38].

Since the NS maximum mass is determined by the high-density region of EoS, a stiffer EoS generates a heavier NS. It is necessary to introduce the extra repulsive mechanism in the QMF scheme, as theoretical efforts are done in the RMF framework in Refs. [3,9–12]. Also, in a recent work of the QMC model [23], besides the usual σ, ω, ρ fields, a nonlinear $\omega - \rho$ term was introduced (with a new coupling parameter Λ_v) in the Lagrangian to correct the stiff behavior of the symmetry energy at large densities. For example, the slope parameter L of the symmetry energy was lowered from 93.59 MeV to 39.04 MeV for $\Lambda_v = 0.1$. As a result, they got a softer nuclear EoS at high densities (which hinders the onset of hyperons) and a harder EoS with hyperons. With the help of the reduction of the attractiveness of Ξ potential U_Ξ, a $2M_\odot$ NS was finally possible in the model. Similar extensions can be done in the QMF model. However, since the maximum mass of the pure NSs is as heavy as $1.88M_\odot$ in the present QMF model, one would not expect that

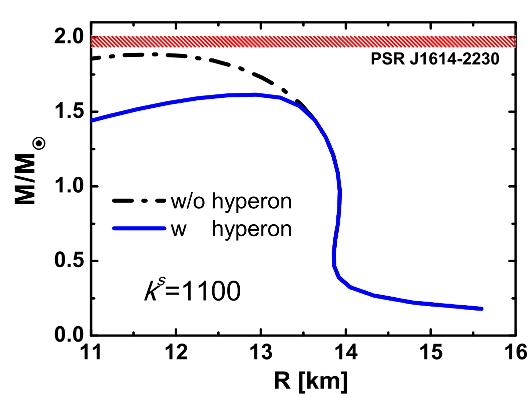

FIG. 6. (Color online) Gravitational masses of NSs are shown as a function of radius, for cases with or without hyperons in the star's core. The recently measured pulsar, PSR J1614-2230, is also indicated with a horizontal shadowed area.

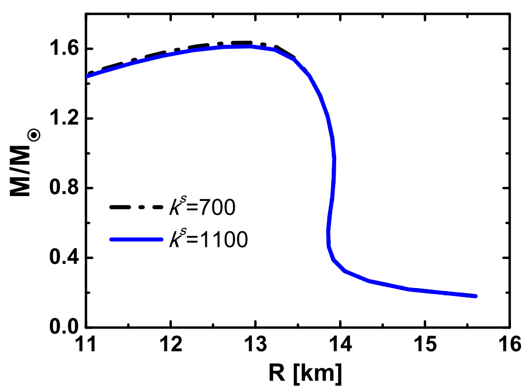

FIG. 7. (Color online) Gravitational masses of hyperon stars are shown as a function of radius for both $k^s = 700$ MeV/fm^2 and $k^s = 1100$ MeV/fm^2 cases.

the corresponding hyperon stars could be heavier than that. This demonstrates the limitations of the present neutron star model.

To discuss the effect of SU(3) symmetry breaking on the NS structure, we also calculate the mass-radius relation of NS with $k^s = 700$ MeV/fm^2. The results are plotted in Fig. 7, compared with the breaking case of $k^s = 1100$ MeV/fm^2. The solid curve is the mass-radius relation considering the SU(3) symmetry breaking, while the dot-dashed curve is SU(3) symmetry conservation at the quark level. The maximum masses of NS are not much changed in these two cases. They are only slightly lowered in the symmetry-breaking case resulting from more hyperon softening, as indicated in Fig. 4 for various compositions of the matter.

IV. SUMMARY AND FUTURE PERSPECTIVES

We extended the QMF model to study infinite hyperonic matter, which includes the Λ, Σ, and Ξ hyperons. The SU(3) symmetry was broken in the quark level to be consistent with the experimental data of Λ potential at nuclear saturation density, i.e., $U_\Lambda^{(N)} \sim 30$ MeV. Namely, we chose different potential strengths for u, d, and s quarks at quark mean fields. Using such quark potential strengths, the coupling constants between σ mesons and baryons were determined through the effective baryon masses from the Dirac equation of quarks. These coupling constants strongly depended on the density and differed from the results of the quark counting rules supported by SU(3) symmetry. We also chose a slightly larger ω coupling with Σ hyperons, than that of Λ hyperons, to reproduce the presently expected single Σ potential of $U_\Sigma = 30$ MeV at the nuclear saturation density. We could then also obtain a slightly attractive Ξ potential desired in the hypernuclei experiments, which was missing in the previous SU(3) QMF model.

We calculated the properties of NSs with the EQMF model and discussed the SU(3) symmetry-breaking effect on the NS mass. The onset of hyperons is moved ahead using the SU(3) breaking potential, and the fraction of hyperons is increased in the star. However, the maximum mass of NSs was found to be almost unchanged, compared with the case when we kept the SU(3) symmetry at the quark level. The maximum mass of NSs approaches $1.62M_\odot$ with hyperons and $1.88M_\odot$ without hyperons. These results could not explain the $2M_\odot$ NS observations.

In order to resolve the limitations of the model, one has to readjust all the QMF parameters from reproducing finite nuclei data in order to achieve a proper new parameter set to fulfill the $2M_\odot$ constraint. There is also a possibility that the phase transitions to a strongly interacting quark matter in the star's core that can support $2M_\odot$ gravitational mass. These topics will be studied in our future works.

ACKNOWLEDGMENTS

We would like to thank Prof. H. Shen and Prof. M. Oka for valuable discussions. The work was supported by the National Natural Science Foundation of China (Contracts No. 11175219, No. 10875151, and No. 10905048), the Major State Basic Research Developing Program of China (No. 2007CB815004), the Knowledge Innovation Project (No. KJCX2-EW-N01) of the Chinese Academy of Sciences, the Chinese Academy of Sciences Visiting Professorship for Senior International Scientists (Grant No. 2009J2-26), and the China Postdoctoral Foundation (Grant No. Science 2012M520100).

[1] J. Schaffner-Bielich and A. Gal, Phys. Rev. C **62**, 034311 (2000).
[2] A. Li, W. Zuo, A.-J. Mi, and G. F. Burgio, Chin. Phys. **16**, 1934 (2007).
[3] K. Tsubakihara and A. Ohnishi, Nucl. Phys. A **914**, 438 (2013).
[4] J. Schaffner, C. Greiner, and H. Stocker, Phys. Rev. C **46**, 322 (1992).
[5] I. Vidana, A. Polls, A. Ramos, L. Engvik, and M. Hjorth-Jensen, Phys. Rev. C **62**, 035801 (2000).
[6] J. Schaffner-Bielich, M. Hanauske, H. Stocker, and W. Greiner, Phys. Rev. Lett. **89**, 171101 (2002).
[7] H. Shen, F. Yang, and H. Toki, Prog. Theor. Phys. **115**, 325 (2006).
[8] W. H. Long, B. Y. Sun, K. Hagino, and H. Sagawa, Phys. Rev. C **85**, 025806 (2012).
[9] S. Weissenborn, D. Chatterjee, and J. Schaffner-Bielich, Nucl. Phys. A **881**, 62 (2012); Phys. Rev. C **85**, 065802 (2012).
[10] G. Colucci and A. Sedrakian, Phys. Rev. C **87**, 055806 (2013).
[11] T. Miyatsu, M.-K. Cheoun, and K. Saito, Phys. Rev. C **88**, 015802 (2013).
[12] C. Providencia and A. Rabhi, Phys. Rev. C **87**, 055801 (2013).
[13] H. Shen, Phys. Rev. C **65**, 035802 (2002).
[14] S. Fleck, W. Bentz, K. Shimizu, and K. Yazaki, Nucl. Phys. A **510**, 731 (1990).
[15] K. Saito and A. W. Thomas, Phys. Lett. B **327**, 9 (1994); **335**, 17 (1994); **363**, 157 (1995).
[16] P. A. M. Guichon, K. Saito, E. Rodionov, and A. W. Thomas, Nucl. Phys. A **601**, 349 (1996).

[17] K. Saito, K. Tsushima, and A. W. Thomas, Nucl. Phys. A **609**, 339 (1996); Phys. Rev. C **55**, 2637 (1997); Phys. Lett. B **406**, 287 (1997).

[18] P. K. Panda, A. Mishra, J. M. Eisenberg, and W. Greiner, Phys. Rev. C **56**, 3134 (1997).

[19] P. K. Panda, R. Sahu, and C. Das, Phys. Rev. C **60**, 038801 (1999).

[20] P. K. Panda, G. Krein, D. P. Menezes, and C. Providencia, Phys. Rev. C **68**, 015201 (2003).

[21] P. K. Panda, D. P. Menezes, and C. Providencia, Phys. Rev. C **69**, 025207 (2004).

[22] P. Yue and H. Shen, Phys. Rev. C **74**, 045807 (2006).

[23] P. K. Panda, A. M. S. Santos, D. P. Menezes, and C. Providencia, Phys. Rev. C **85**, 055802 (2012).

[24] H. Shen and H. Toki, Phys. Rev. C **61**, 045205 (2000).

[25] H. Shen and H. Toki, Nucl. Phys. A **707**, 469 (2002).

[26] P. Wang, Z. Y. Zhang, Y. W. Yu, R. K. Su, and H. Q. Song, Nucl. Phys. A **688**, 791 (2001).

[27] P. Wang, D. B. Leinweber, A. W. Thomas, and A. G. Williams, Nucl. Phys. A **744**, 273 (2004).

[28] P. Wang, S. Lawley, D. B. Leinweber, A. W. Thomas, and A. G. Williams, Phys. Rev. C **72**, 045801 (2005).

[29] H. Toki, U. Meyer, A. Faessler, and R. Brockmann, Phys. Rev. C **58**, 3749 (1998).

[30] P. Wang, H. Guo, Z. Y. Zhang, Y. W. Yu, R. K. Su, and H. Q. Song, Nucl. Phys. A **705**, 455 (2002).

[31] P. Wang, V. E. Lyubovitskij, Th. Gutsche, and A. Faessler, Phys. Rev. C **67**, 015210 (2003).

[32] P. Wang, D. B. Leinweber, A. W. Thomas, and A. G. Williams, Phys. Rev. C **70**, 055204 (2004).

[33] P. Wang, D. B. Leinweber, A. W. Thomas, and A. G. Williams, Nucl. Phys. A **748**, 226 (2005).

[34] R. E. Chrien and C. B. Dover, Annu. Rev. Nucl. Part. Sci. **39**, 113 (1989); H. Bandō, T. Motoba, and J. Žofka, Int. J. Mod. Phys. A **05**, 4021 (1990).

[35] H. Takahashi, J. K. Ahn, H. Akikawa, S. Aoki, K. Arai, S. Y. Bahk, K. M. Baik, B. Bassalleck, J. H. Chung, D. H. Davies *et al.*, Phys. Rev. Lett. **87**, 212502 (2001).

[36] P. Khaustov *et al.* (The AGS E885 Collaboration), Phys. Rev. C **61**, 054603 (2000).

[37] E. Hiyama, Y. Yamamoto, T. Motoba, Th. A. Rijken, and M. Kamimura, Phys. Rev. C **78**, 054316 (2008).

[38] Th. A. Rijken, M. M. Nagels, and Y. Yamamoto, Prog. Theor. Phys. Suppl. **185**, 14 (2010).

[39] Th. A. Rijken, M. M. Nagels, and Y. Yamamoto, Few-Body Syst. **54**, 801 (2013).

[40] Y. Yamamoto, E. Hiyama, and Th. A. Rijken, Few-Body Syst. **54**, 1267 (2013).

[41] P. Guichon, Phys. Lett. B **200**, 235 (1988).

[42] B. D. Serot and J. D. Walecka, Adv. Nucl. Phys. **16**, 1 (1986).

[43] T. De. Grand, R. L. Jaffe, K. Johnson, and J. Kiskis, Phys. Rev. D **12**, 2060 (1975).

[44] N. Isgur and G. Karl, Phys. Rev. D **18**, 4187 (1978).

[45] J. N. Hu, A. Li, H. Shen, and H. Toki, Progr. Theor. Exp. Phys. 013D02 (2014).

[46] R. C. Tolman, Phys. Rev. **55**, 364 (1939).

[47] J. R. Oppenheimer and G. M. Volkoff, Phys. Rev. **55**, 374 (1939).

[48] S. L. Shapiro and S. A. Teukosky, *Black Holes, White Dwarfs, and Neutron Stars* (John Wiley, New York, 1983).

[49] J. W. Negele and D. Vautherin, Nucl. Phys. A **207**, 298 (1973).

[50] R. Feynman, F. Metropolis, and E. Teller, Phys. Rev. **75**, 1561 (1949).

[51] G. Baym, C. Pethick, and D. Sutherland, Astrophys. J. **170**, 299 (1971).

[52] P. B. Demorest, T. Pennucci, S. M. Ransom, M. S. E. Roberts, and J. W. T. Hessels, Nature (London) **467**, 1081 (2010); J. Antoniadis, P. C. C. Freire, N. Wex, T. M. Tauris, R. S. Lynch *et al.*, Science **340**, 6131 (2013).

[53] J. M. Lattimer and M. Prakash, Science **304**, 536 (2004).

[54] H.-J. Schulze, A. Polls, A. Ramos, and I. Vidana, Phys. Rev. C **73**, 058801 (2006).

[55] G. F. Burgio, H.-J. Schulze, and A. Li, Phys. Rev. C **83**, 025804 (2011).

[56] H.-J. Schulze and T. Rijken, Phys. Rev. C **84**, 035801 (2011).